LASER ABLATION

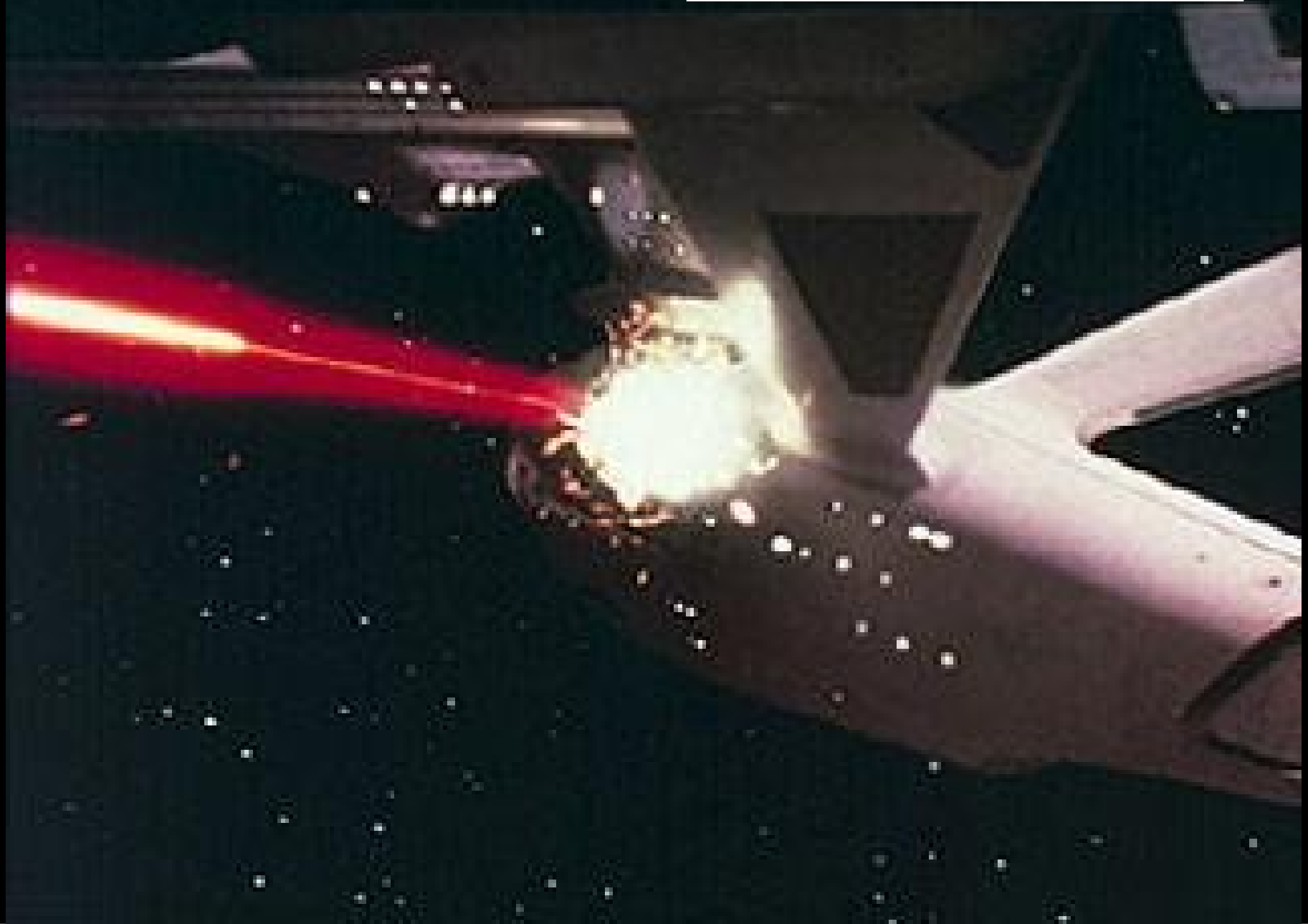

Laser Ablation ICP-MS

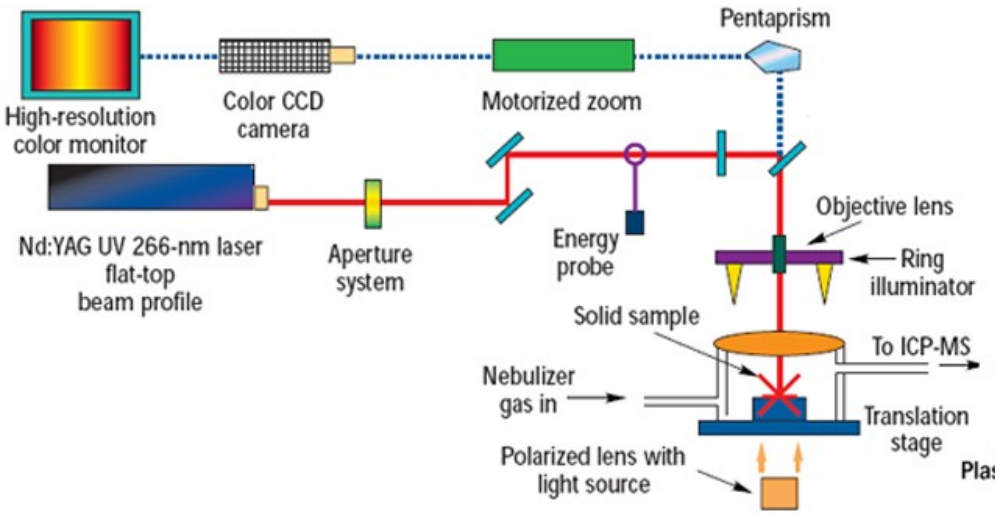

CETAC LSX 500

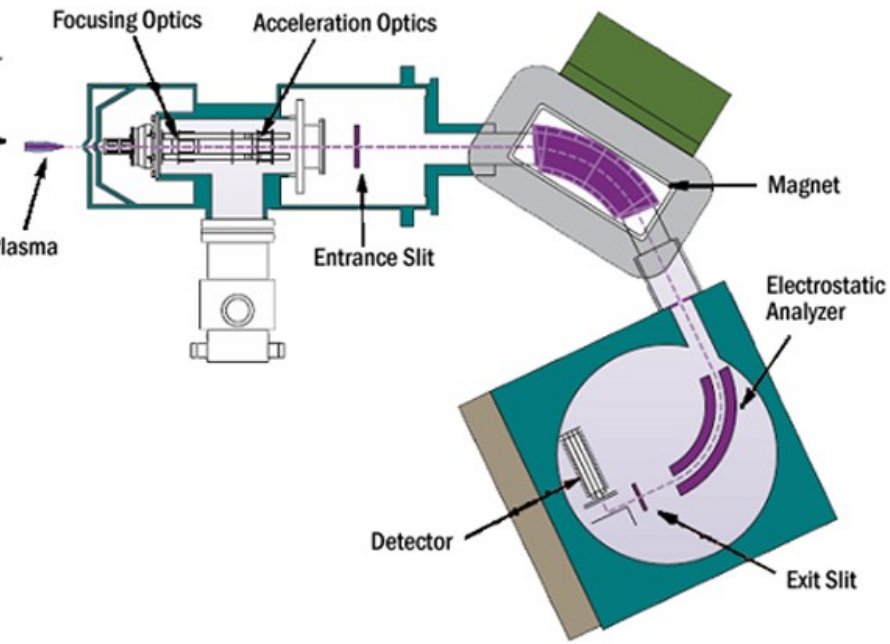

Thermo Finnigan Element

www.cetac.com

www.thermo.com

“Gold can be melted and recast and is therefore virtually untraceable”

DISTINGUISH GOLD SAMPLES BASED ON TRACE ELEMENTS?

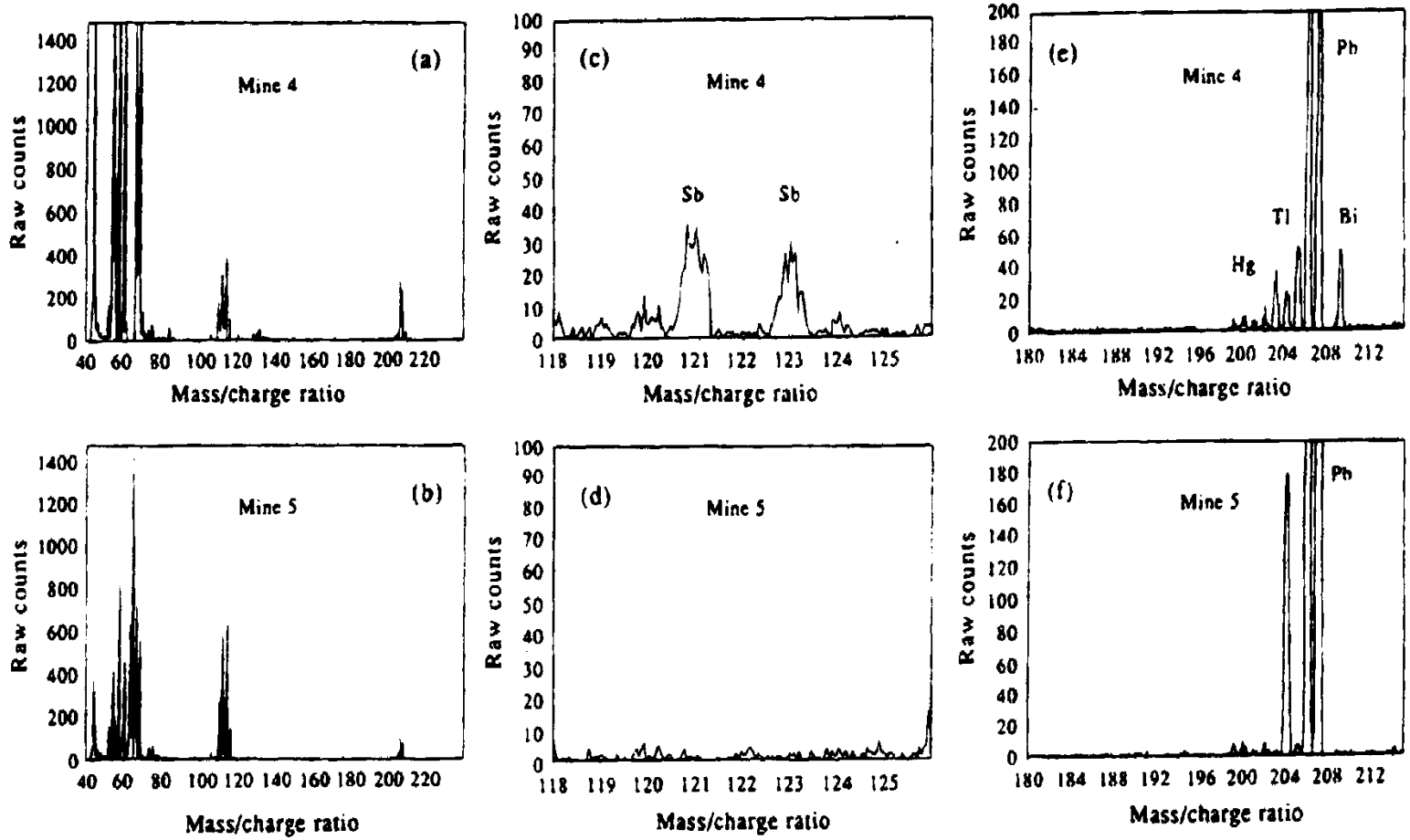

Figure 6. ICP mass spectra of trace impurities in gold from two mines in western Australia. Each sample contains substantial Cd (m/z = 110–116) and Pb (m/z = 204, 206–208). Note that the sample from mine 4 has much more Sb (m/z = 121 and 123), Tl (m/z = 203 and 205), and Bi (m/z = 209) than the sample from mine 5. Reproduced with permission.[41]

Watling et al., Spectrochim. Acta Part B 1994, 49B, 205-219.

DEVELOPMENTS IN LASER ABLATION

GÜNTHER et al., ANAL. CHEM. 2003, 75, 341A; TrAC 2005, 24, 255.

UV LASERS (266 , 213, 193 nm)
HOMOGENIZED BEAM PROFILE
HELIUM TRANSPORT GAS

FRACTIONATION
1. VARIATION OF SIGNAL RATIO vs TIME
AS DIG SINGLE PIT
11.MEAS. SIGNAL RATIOS
DIFFER FROM THOSE IN SAMPLE

SOLUTIONS:
FLAT BOTTOM CRATERS
VERTICAL SIDES
SHORT PULSE (fs) LASER
(RUSSO et al., ANAL. CHEM. 2002, 74, 70A).

PARTICLE SIZE EFFECTS IN LASER ABLATION

GÜNTHER & GUILLONG
JAAS 2002, 17, 831

AESCHLIMAN et al.
JAAS 2003, 18, 1008

Fig. 1 Filtered aerosol of NIST SRM 610 glass after 100 ablation pulses. **a**, **b**) 266 nm laser, 100 μm spot size. Large particles and agglomerates of nano-particles are visible. **c**, **d**) 193 nm laser, 80 μm spot size. Almost exclusively agglomerates of nano-particles are visible; no spherical particles are larger than 200 nm. The pores of the filter are visible in the images as dark areas

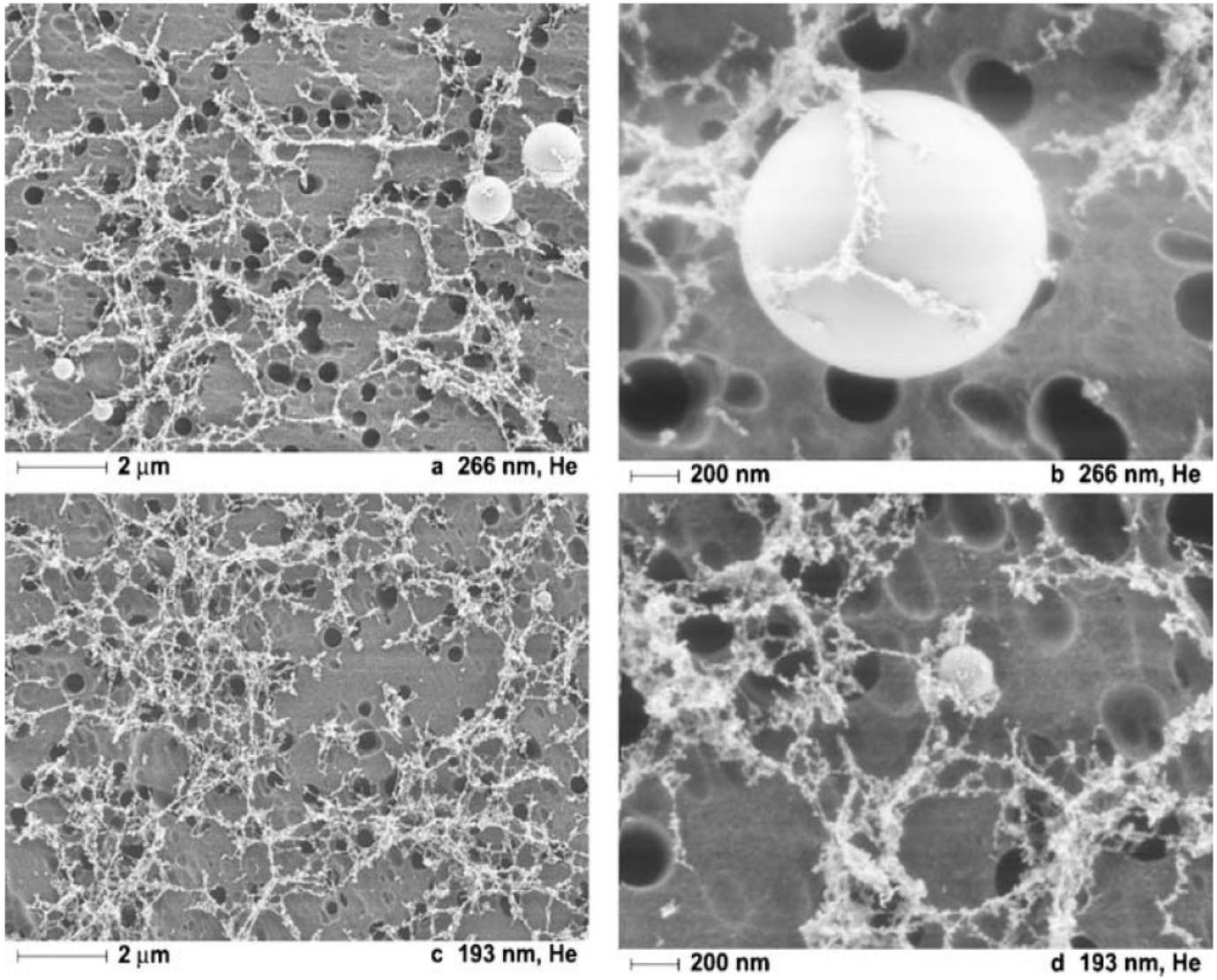

Particles from Ablated Y_2O_3 Pellet

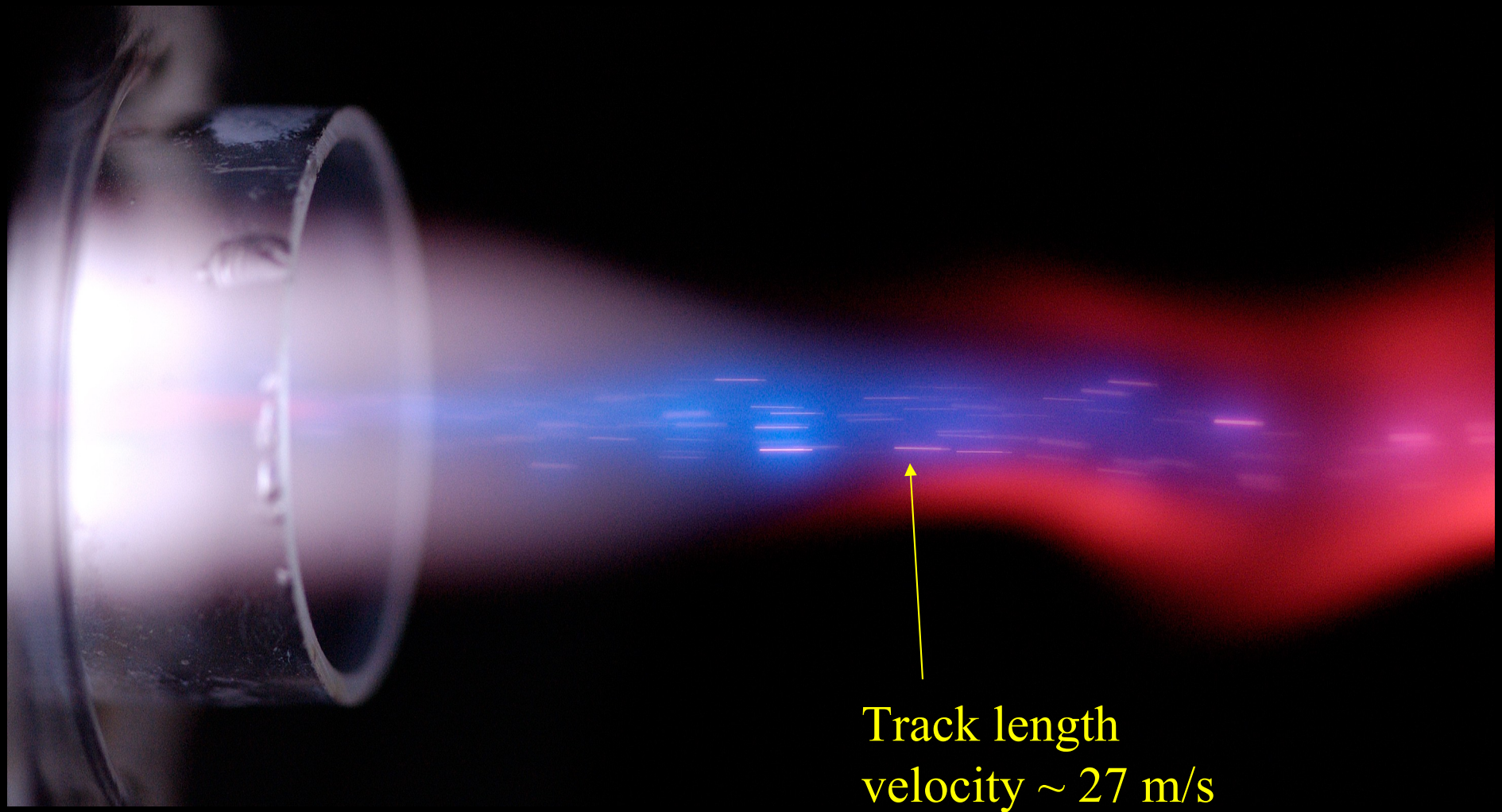

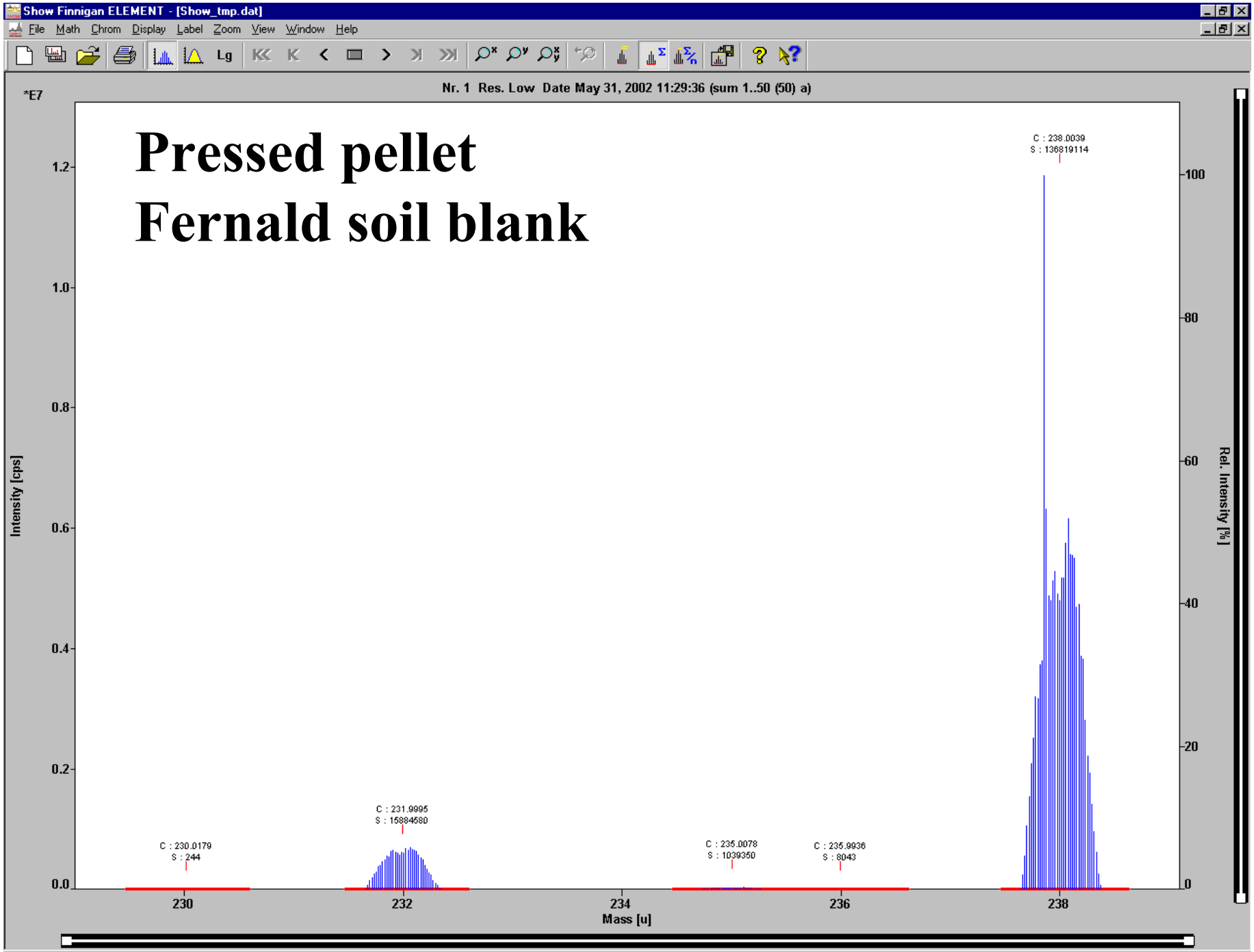
Show Finnigan ELEMENT - [Show_tmp.dat]
File Math Chrom Display Label Zoom View Window Help
Nr. 1 Res. Low Date May 31, 2002 11:29:36 (sum 1..50 (50) a)
*E7
Pressed pellet
Fernald soil blank
C : 238.0039
S : 136819114
C : 231.9995
S : 15884580
C : 230.0179
S : 244
C : 235.0078
S : 1039350
C : 235.9936
S : 8043
Intensity [cps]
Rel. Intensity [%]
Mass [u]
For Help, press F1
NUM

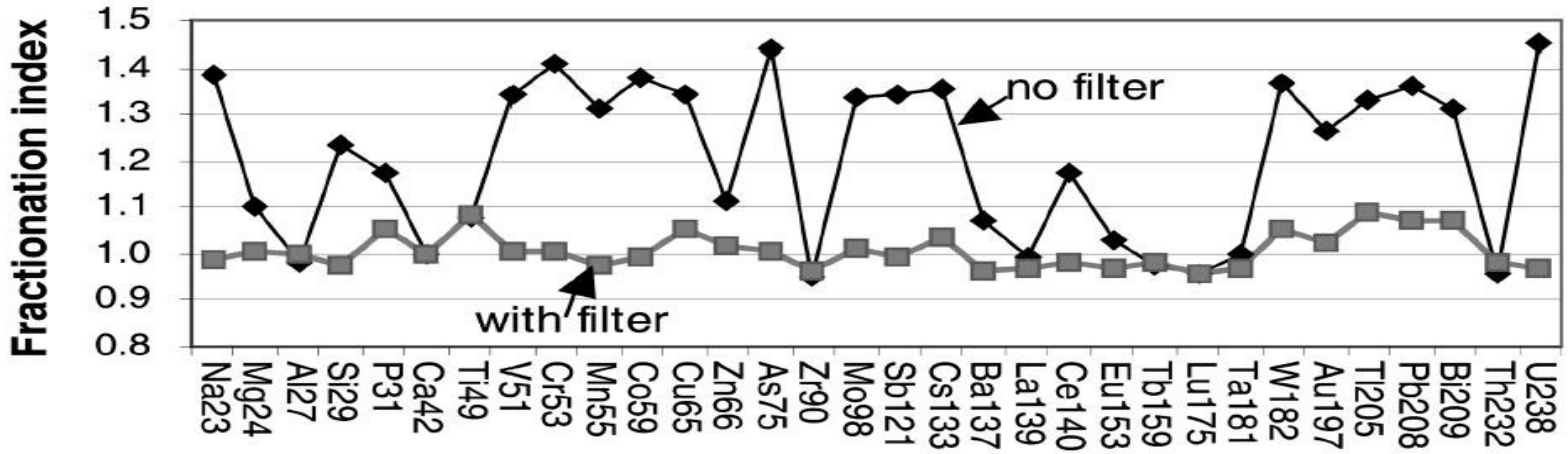

Fig. 8 Fractionation indices calculated from signals acquired in single hole ablation mode. The indices shown are from total aerosol and filtered aerosol introduction into the ICP.

The influence of particle filtering on signal intensities can be assessed using a "fractionation index", which is a measure of the time-dependent variation of elemental ratios during an ablation [$I_{(F)} = (I_{(E)}/I_{(Ca)})_{t2}/(I_{(E)}/I_{(Ca)})_{t1}$, where $I_{(F)}$ is the fractionation index, $I_{(E)}$ the intensity of an element, $I_{(Ca)}$ the intensity of the reference element Ca and $t2$ and $t1$ are the first and second half of the ablation]. In Fig. 8 it can be seen that, for a wide range of elements, filtering causes the time-dependent variation of elemental ratios to disappear.

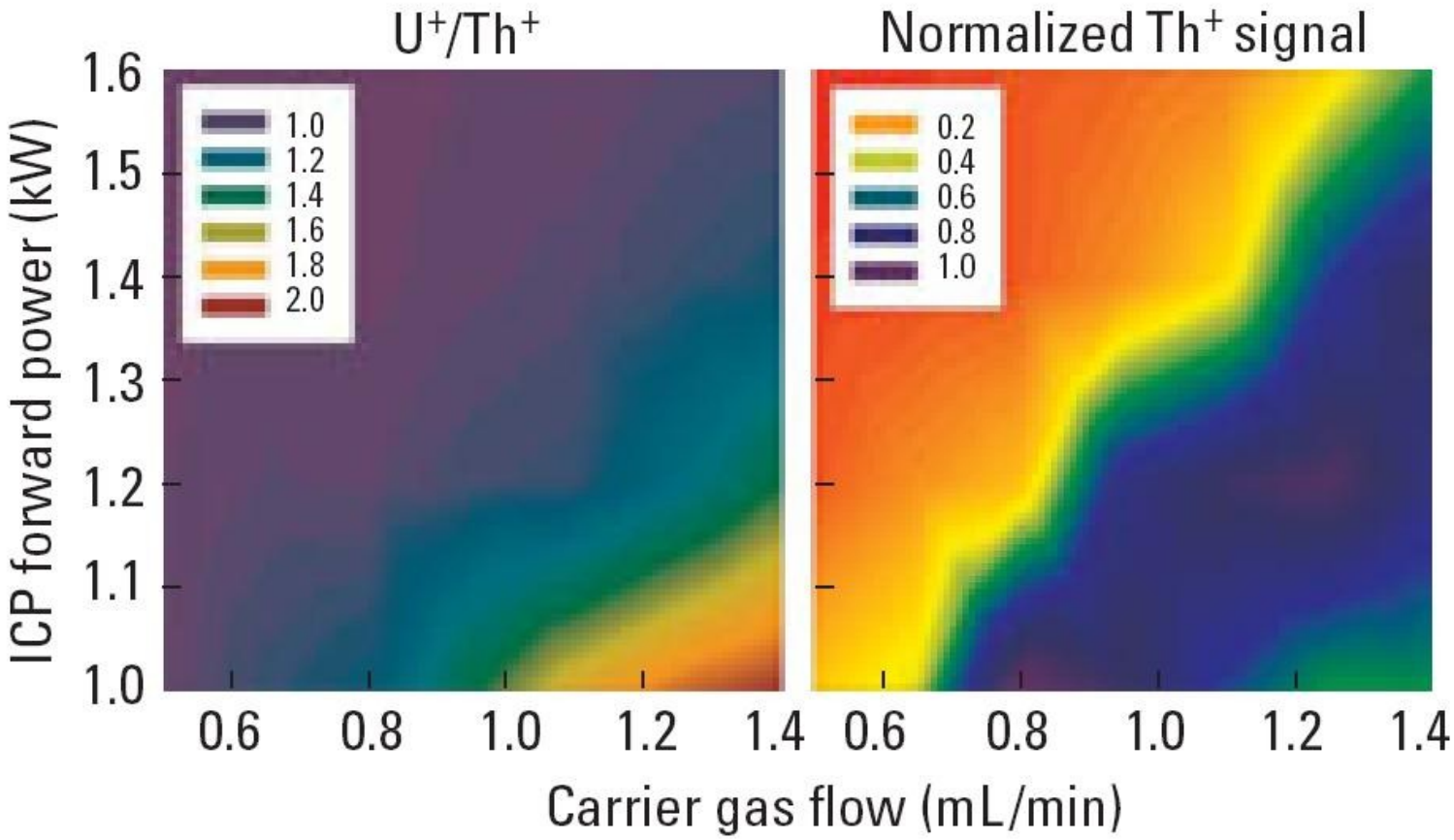

FIGURE 4. The influence of plasma power and carrier gas flow on the intensity ratio for uranium and thorium and the normalized Th^+ signal. The diagrams indicate that the most robust plasma conditions are achievable under compromised sensitivity conditions (loss of 50% thorium intensity).

SINGLE SPOT ABLATION

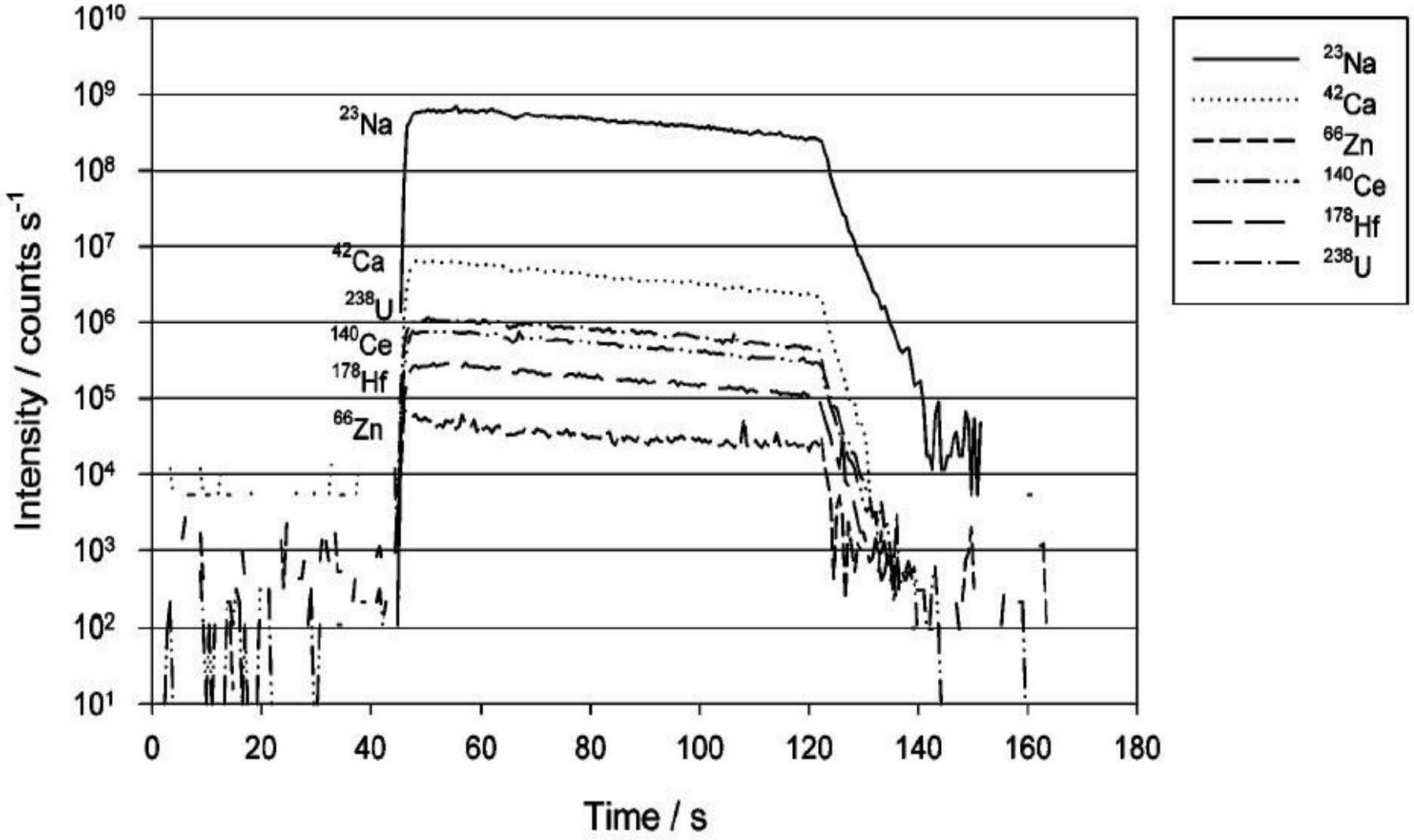

FEMTOSECOND LASER ABLATION

RUSSO et al.
JAAS 2002, 17, 1072.
ANAL. CHEM. 2003, 75, 6184
2004, 76, 379.

Femtosecond Laser Ablation

- Nanosecond laser ablation is partly a thermal process
- Differences in the vaporization properties of elements leads to elemental fractionation
- With femtosecond pulses, the ablation process occurs by a mechanism far less dependent on thermal effects. Melting is not observed with pulse widths < 1 ps.

Crater Profiles

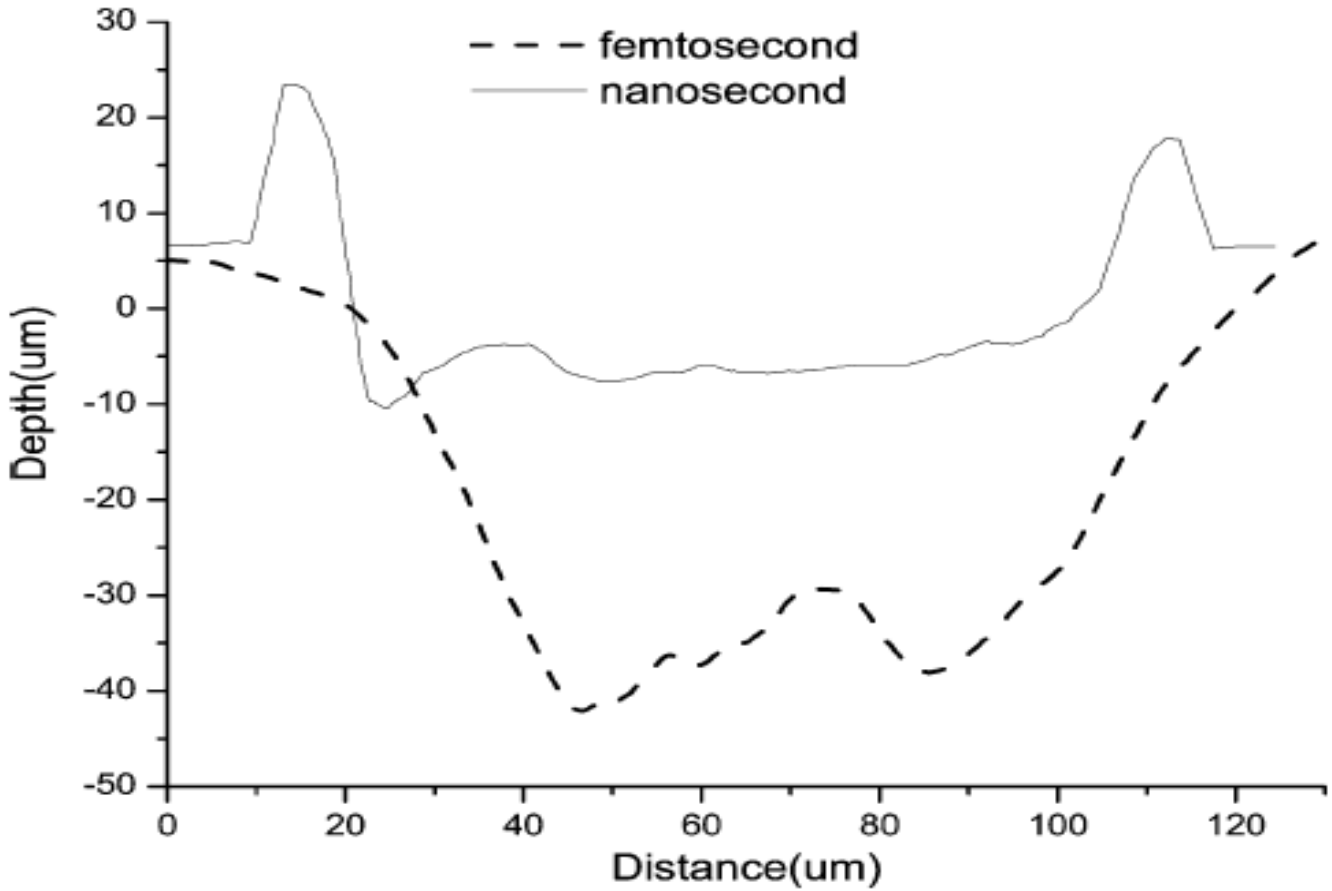

Crater profiles for 100 fs and 4 ns lasers after 50 pulses

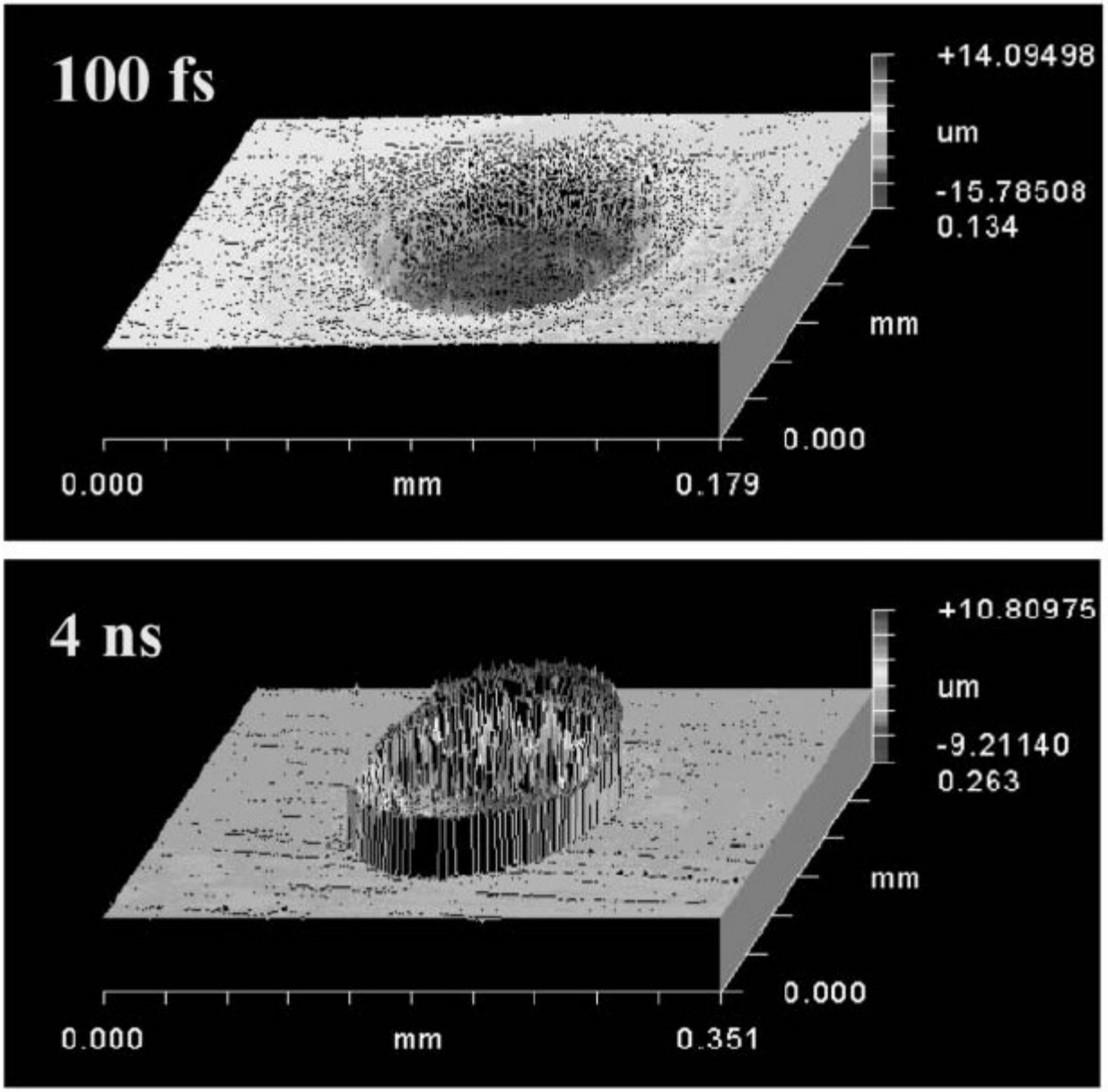

Fig. 5 Femtosecond and nanosecond pulsed laser ablated craters in metal sample.

UV fs LASER ABLATION
INGO HORN
UNIV. HANNOVER

Geochimica et Cosmochimica Acta 70 (2006) 3677–3688

In situ iron isotope ratio determination using UV-femtosecond laser ablation with application to hydrothermal ore formation processes

Ingo Horn [a,*], Friedhelm von Blanckenburg [a], Ronny Schoenberg [a], Grit Steinhoefel [a], Gregor Markl [b]

[a] *Universität Hannover, Institut für Mineralogie, Callinstr. 3, D-30167 Hannover, Germany*
[b] *Universität Tuebingen, Institut für Geowissenschaften, Wilhelmstr. 56, D-72074 Tüebingen, Germany*

fs-laser ablation system

Laser

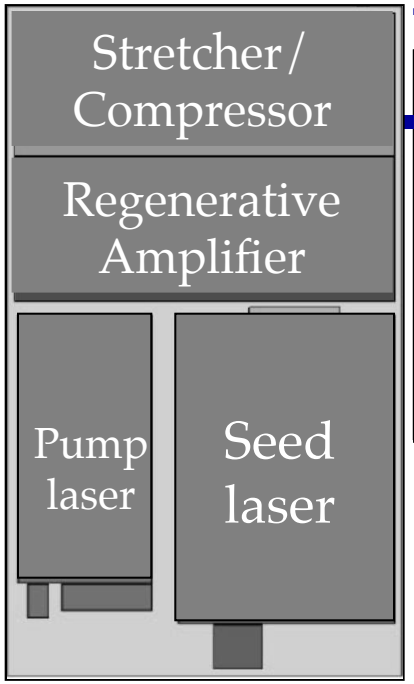

Optics

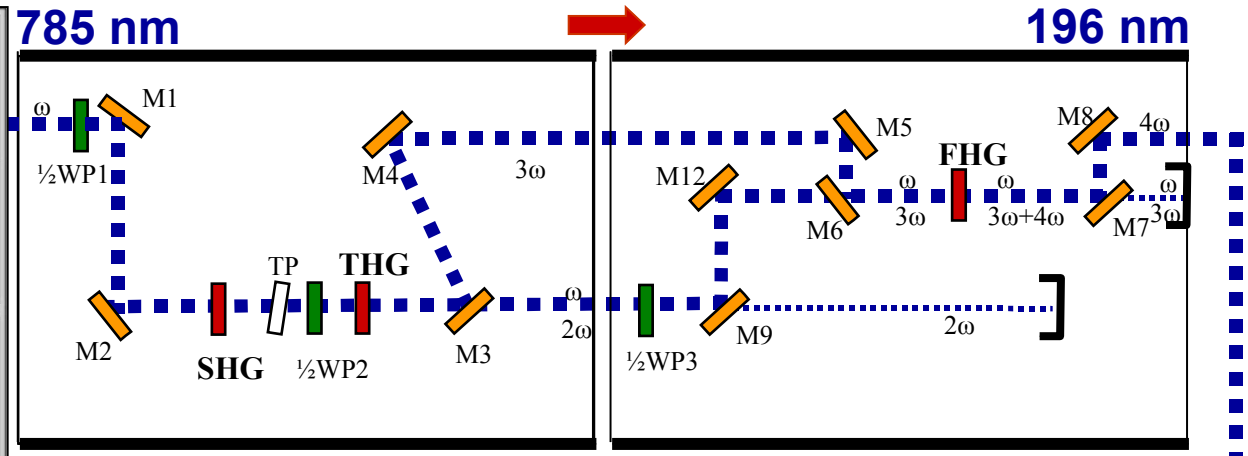

100fs=0.0000000000001sec.

By comparison, if traveling at the speed of light for 100 fs you would only just cover about 30 μm in distance.

MC-ICP-MS or ICP-OES

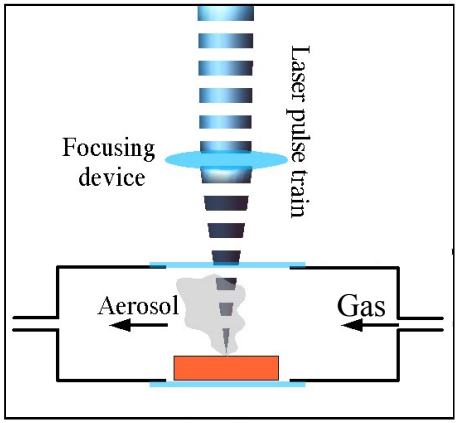

Sample cell

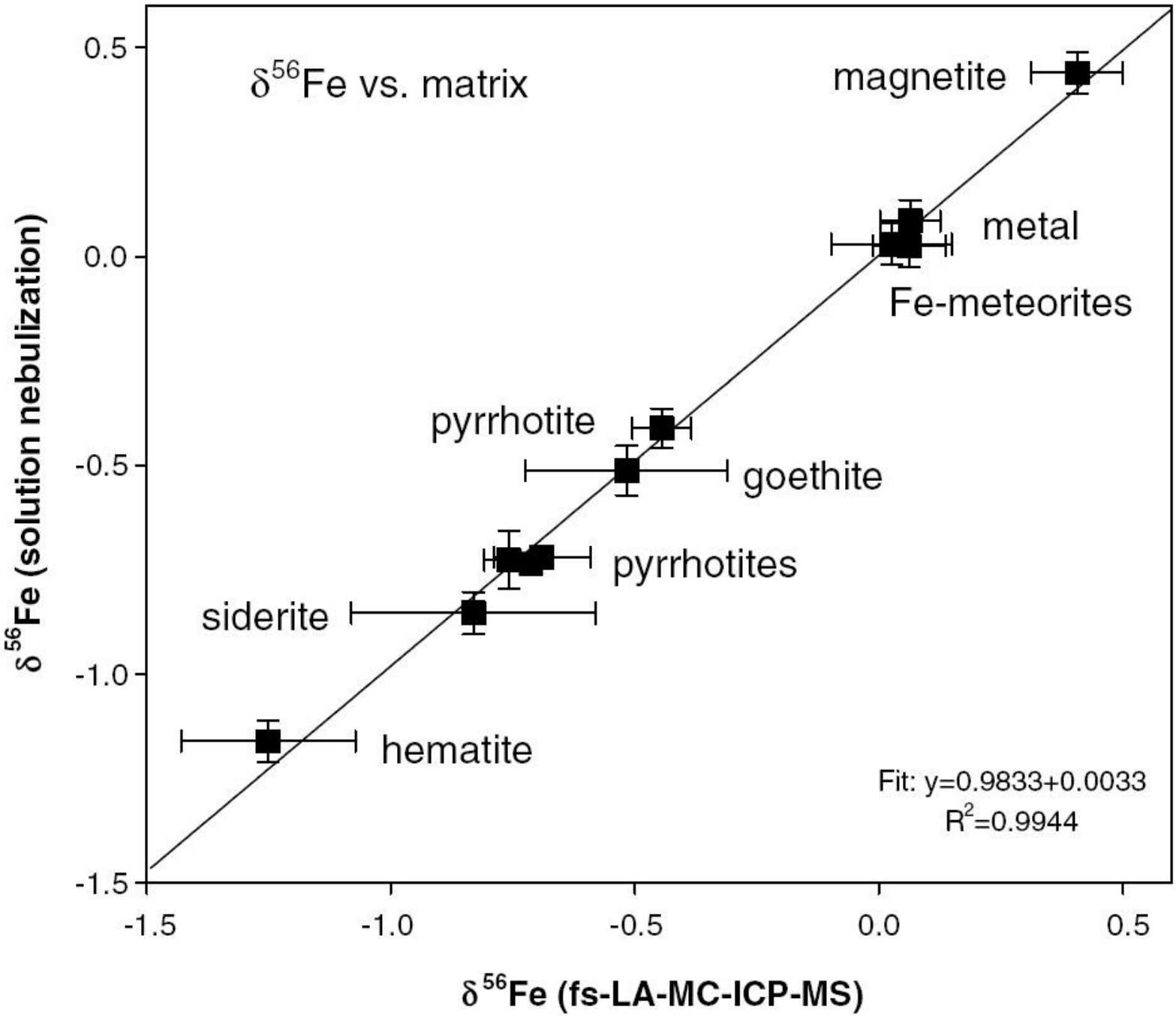
δ56Fe vs. matrix
magnetite
metal
Fe-meteorites
pyrrhotite
goethite
pyrrhotites
siderite
hematite
Fit: y=0.9833+0.0033
R2=0.9944
0.5
0.0
-0.5
-1.0
-1.5
-1.5
-1.0
-0.5
0.0
0.5
δ56Fe (solution nebulization)
δ56Fe (fs-LA-MC-ICP-MS)

<u>CALIBRATE LASER ABLATION?</u>

COMPENSATE FOR MATRIX DEPENDENCE OF ABLATION PROCESS

MATCHED STANDARDS

MEAS. ANALYTE REL. TO MINOR ISOTOPE OF ELEMENT AT KNOWN CONCENTRATION

CALIBRATE REL. TO SOLUTION AEROSOL?
BECKER JAAS 2001, 16, 602
AESCHLIMAN JAAS 2003, 18, 872-877.

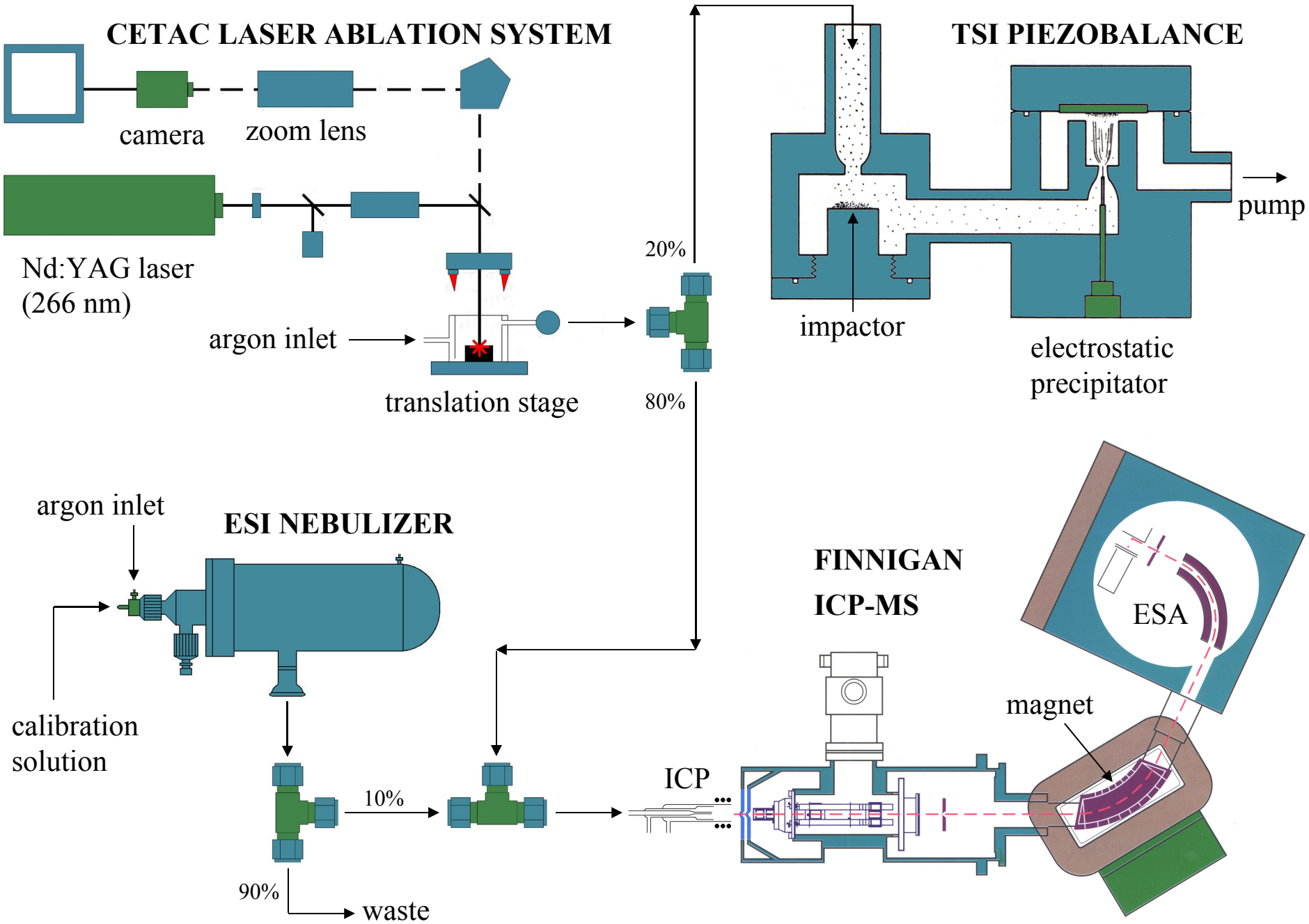
CETAC LASER ABLATION SYSTEM
camera
zoom lens
Nd:YAG laser
(266 nm)
argon inlet
translation stage
20%
80%
TSI PIEZOBALANCE
impactor
electrostatic
precipitator
pump
argon inlet
ESI NEBULIZER
calibration
solution
10%
90%
waste
ICP
FINNIGAN
ICP-MS
ESA
magnet

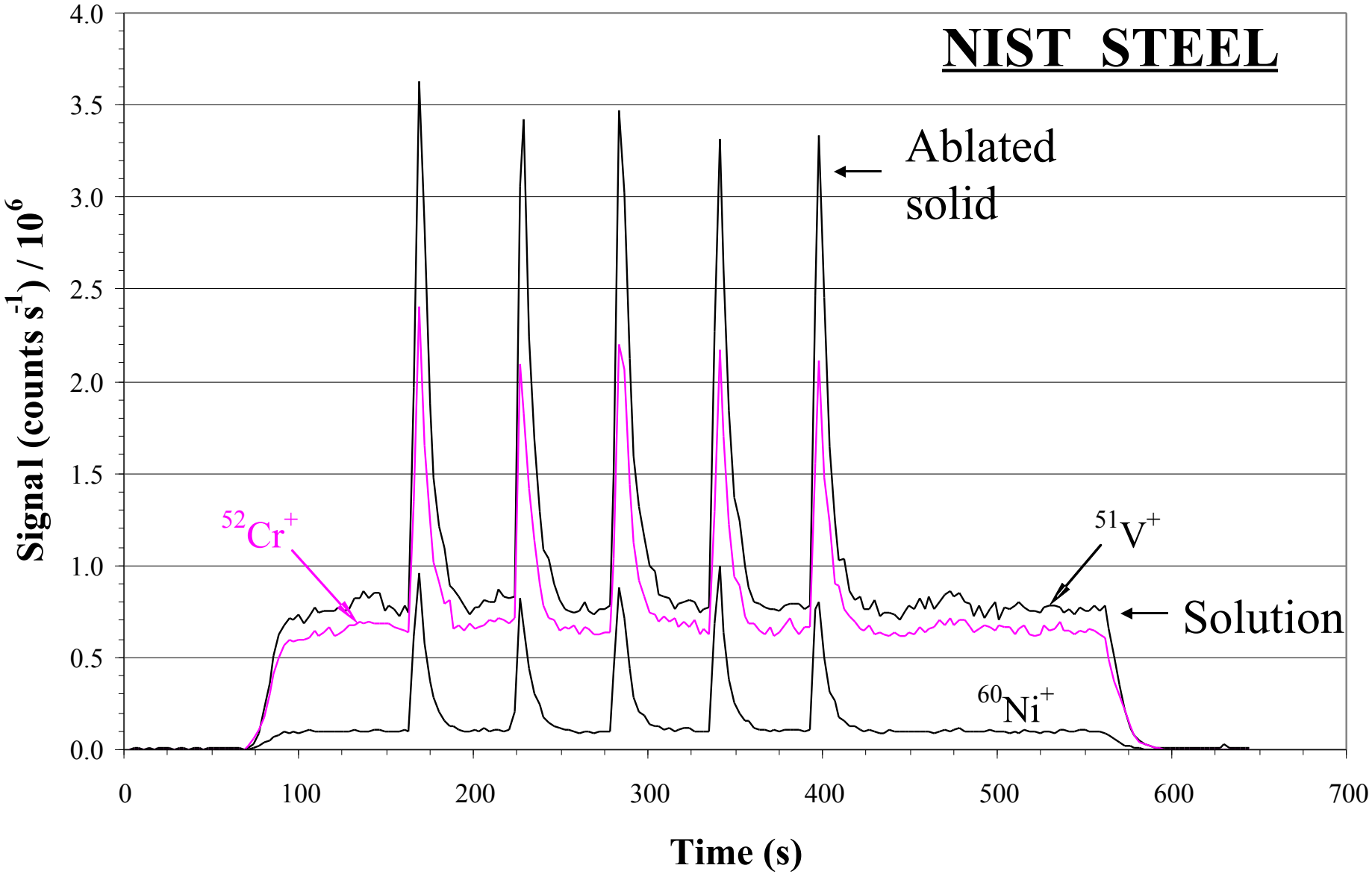
NIST STEEL
Ablated solid
Solution
$^{52}Cr^+$
$^{51}V^+$
$^{60}Ni^+$
Signal (counts s^{-1}) / 10^6
Time (s)
4.0
3.5
3.0
2.5
2.0
1.5
1.0
0.5
0.0
0
100
200
300
400
500
600
700

Calibration of LA-ICP-MS with Dried Solution Aerosols

- Simultaneous introduction of particles from a LA cell and desolvated aerosol particles from a micro-flow nebulizer

$$S_{total} = S_{solid} + S_{solution}$$
$$= R_{X,solid}\, T_{LA} t [X]_{solid} + R_{X,soln}\, V T_{neb} [X]_{soln}$$

R_X	isotope-specific response factor (signal/ng X)
T_{LA}	transport from LA cell (ng solid/s)
t	time of ablation transient (s)
$[X]_{solid}$	concentration of isotope in solid (ng X/ng solid)
V	volume of solution injected to ICP (L)
T_{neb}	nebulizer efficiency
$[X]_{soln}$	isotopic concentration in solution standard (ng X/L)

NIST 612 Glass (13 Elements, 5 Replicates)

- Particle transport from the LA cell was measured using a piezoelectric microbalance
- Each replicate was generated by firing 50 laser shots per localized spot on the sample
- A two-point calibration plot for each replicate was prepared and an average calculated
- All elements were measured in medium resolution ($R = m/\Delta m = 4000$)

		CONCENTRATION (ppm)			
		MEASURED		CERTIFIED	Relative Diff. (%)
Mn	($^{55}Mn^+$)	40.8	7.9	(39.6)	3.0
Fe	($^{56}Fe^+$)	51.6	6.1	51	1.2
Co	($^{59}Co^+$)	36.0	4.7	(35.5)	1.4
Ni	($^{60}Ni^+$)	39.2	4.7	38.8	1.0
Cu	($^{63}Cu^+$)	38.5	6.7	(37.7)	2.1
Ba	($^{138}Ba^+$)	41.6	5.5	(41)	1.5
Nd	($^{146}Nd^+$)	36.2	2.6	(36)	0.56
Sm	($^{147}Sm^+$)	39.5	4.7	(39)	1.3
Eu	($^{151}Eu^+$)	36.5	4.7	(36)	1.4
Dy	($^{161}Dy^+$)	35.1	2.5	(35)	0.29
Er	($^{166}Er^+$)	39.3	4.2	(39)	0.77
Tl	($^{205}Tl^+$)	15.8	1.6	(15.7)	0.64
Pb	($^{208}Pb^+$)	39.2	5.8	38.57	1.6

NIST 1264a Steel (8 Elements)

- 266 nm QUAD. Nd:YAG LASER, CETAC LSX-100
- AVG. 30 SPOTS, TWO-POINT STD. ADDNS.
- 50 SHOTS PER SPOT, MED. RES.
- PARTICLE TRANSPORT MEAS. WITH MICROBALANCE

	CONCENTRATION (wt %)		
	MEAS.		CERT. (INFO)
V ($^{51}V^{+}$)	0.119	0.029	0.106
Cr ($^{52}Cr^{+}$)	0.073	0.012	0.066
Co ($^{59}Co^{+}$)	0.156	0.017	0.150
Ni ($^{60}Ni^{+}$)	0.143	0.017	0.142
Cu ($^{63}Cu^{+}$)	0.248	0.040	0.250
W ($^{184}W^{+}$)	0.107	0.027	0.102
Pb ($^{208}Pb^{+}$)	0.056	0.055	0.024
Bi ($^{209}Bi^{+}$)	0.0016	0.0032	(0.0009)

NIST 1264a Steel (8 Elements)

- 193 nm ArF LASER
- AVG. 3 SPOTS, TWO-POINT STD. ADDNS.
- 50 SHOTS PER SPOT, MED. RES.
- PARTICLE TRANSPORT MEAS. WITH MICROBALANCE

	CONCENTRATION (wt %)		
	MEAS.		CERT. (INFO)
V ($^{51}V^{+}$)	0.115	0.011	0.106
Cr ($^{52}Cr^{+}$)	0.078	0.036	0.066
Co ($^{59}Co^{+}$)	0.137	0.035	0.150
Ni ($^{60}Ni^{+}$)	0.139	0.108	0.142
Cu ($^{63}Cu^{+}$)	0.277	0.201	0.250
W ($^{184}W^{+}$)	0.108	0.013	0.102
Pb ($^{208}Pb^{+}$)	0.021	0.004	0.024
Bi ($^{209}Bi^{+}$)	0.0006	0.0001	(0.0009)

Multivariate Analysis in LA-ICP-MS

Laser Ablation of NIST 1224 Steel

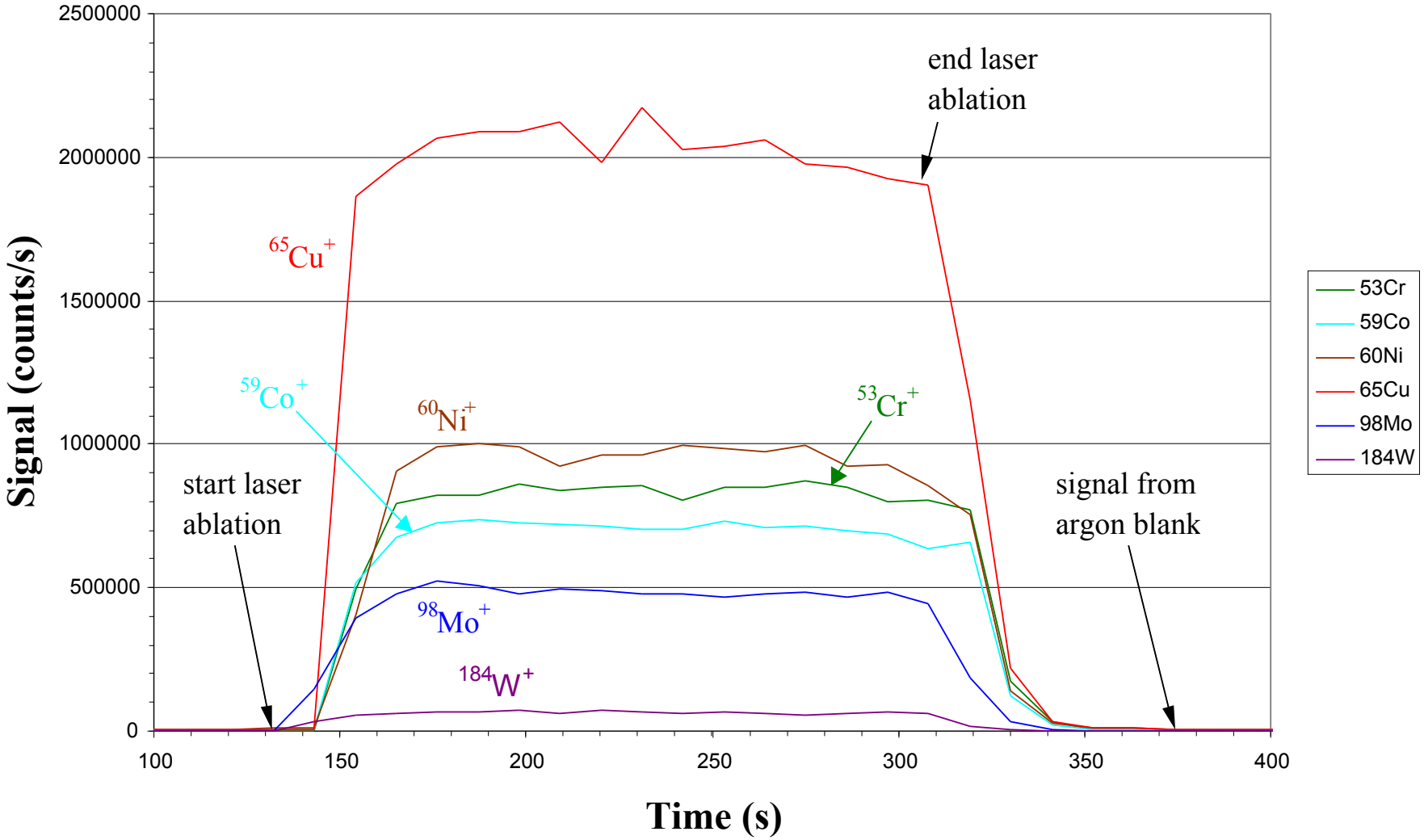

STEEL SAMPLES

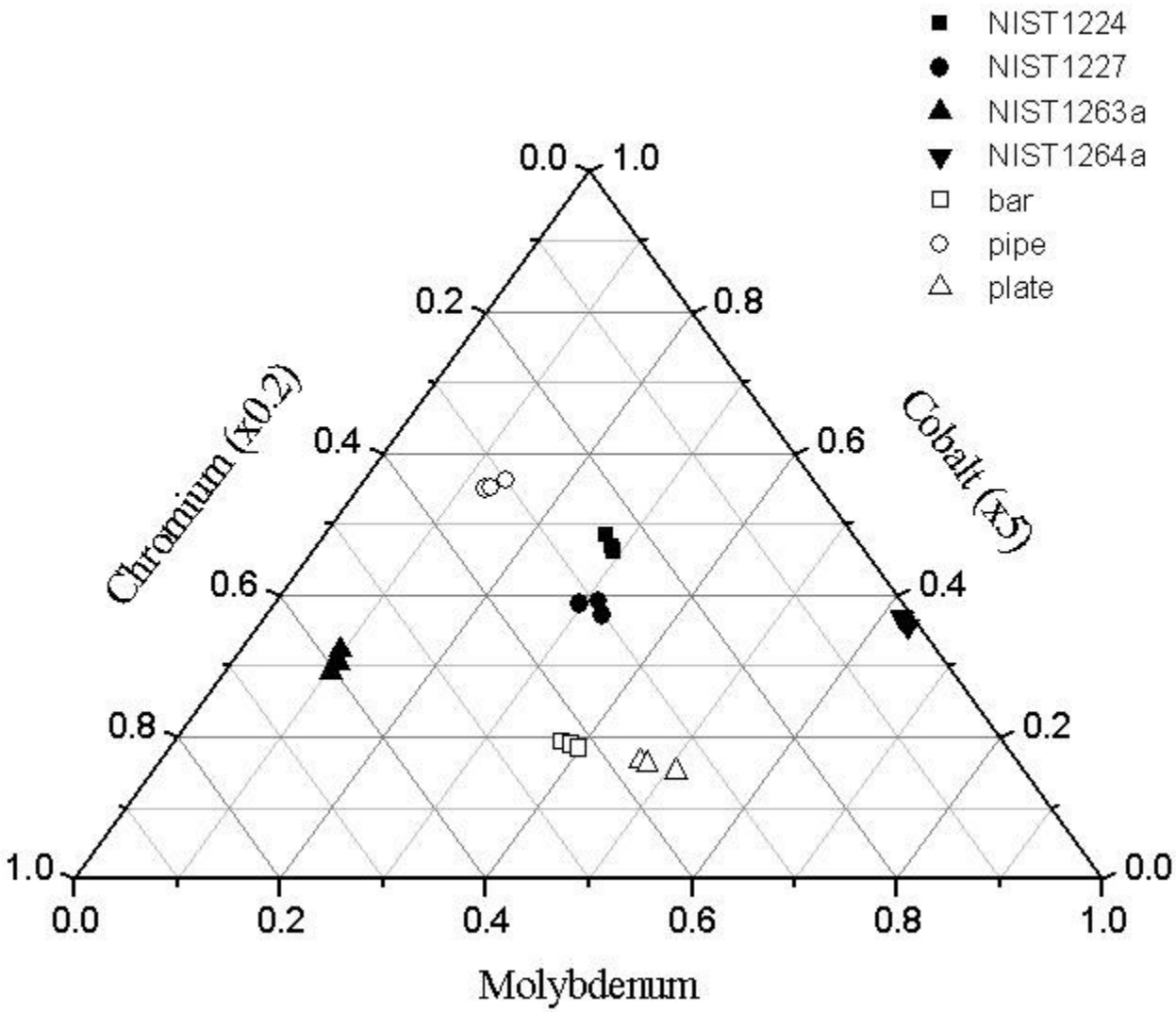

Principal Component Analysis

- Eigenvector decomposition of covariance matrix
- Matlab toolbox developed by Eigenvector Research, Inc.
- “Traditionally” applied to IR spectra
- Used to extract reduced dimension “factors” that describe trends and similarities/dissimilarities in data from multi-component spectra

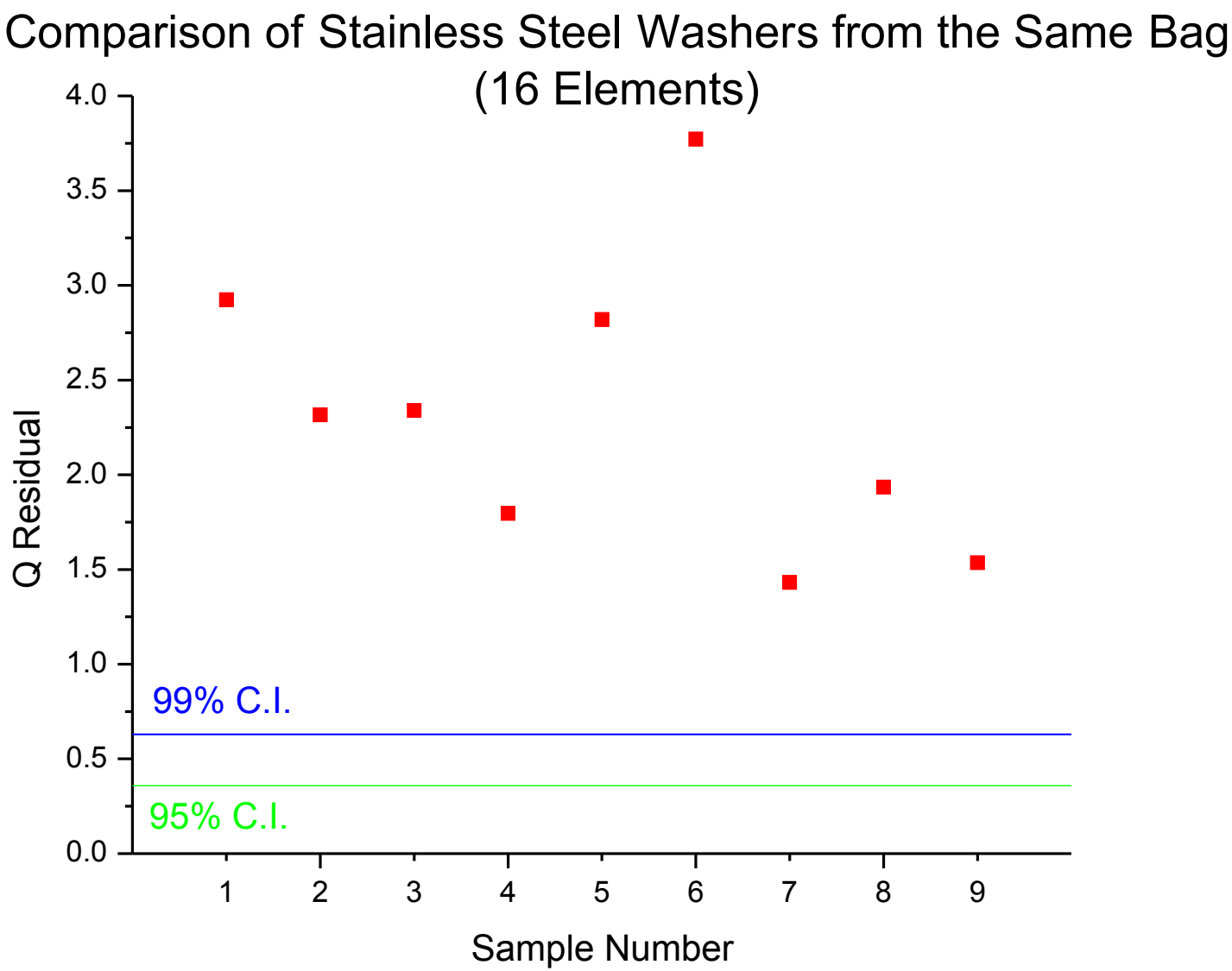
Comparison of Stainless Steel Washers from the Same Bag
(16 Elements)
Q Residual
4.0
3.5
3.0
2.5
2.0
1.5
1.0
0.5
0.0
99% C.I.
95% C.I.
1
2
3
4
5
6
7
8
9
Sample Number

Comparison of Two Stainless Steel Washers from the Same Box
(19 elements)

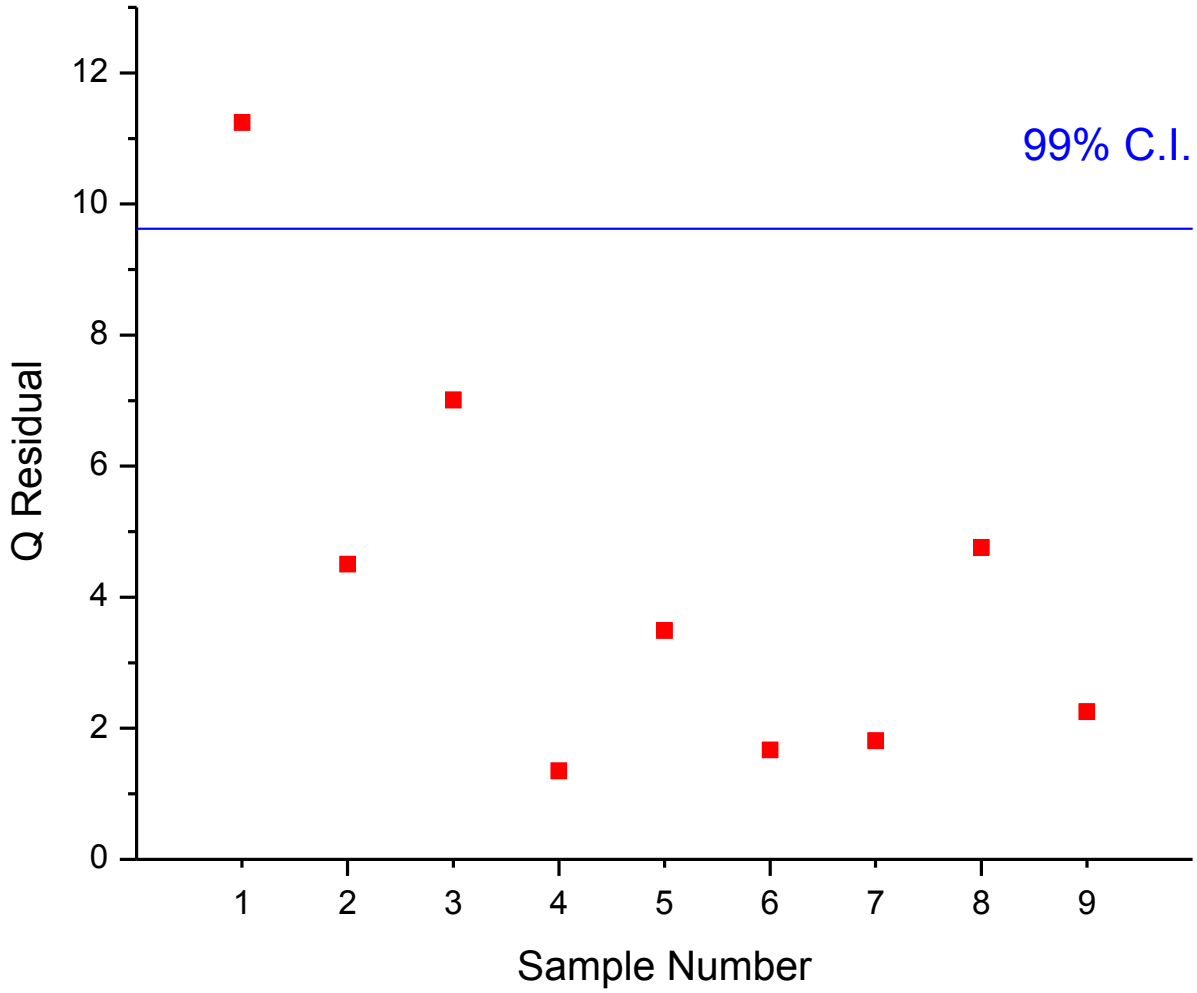

Chemometric Comparison of Seven Carbon Steels
(25 Isotope Model)

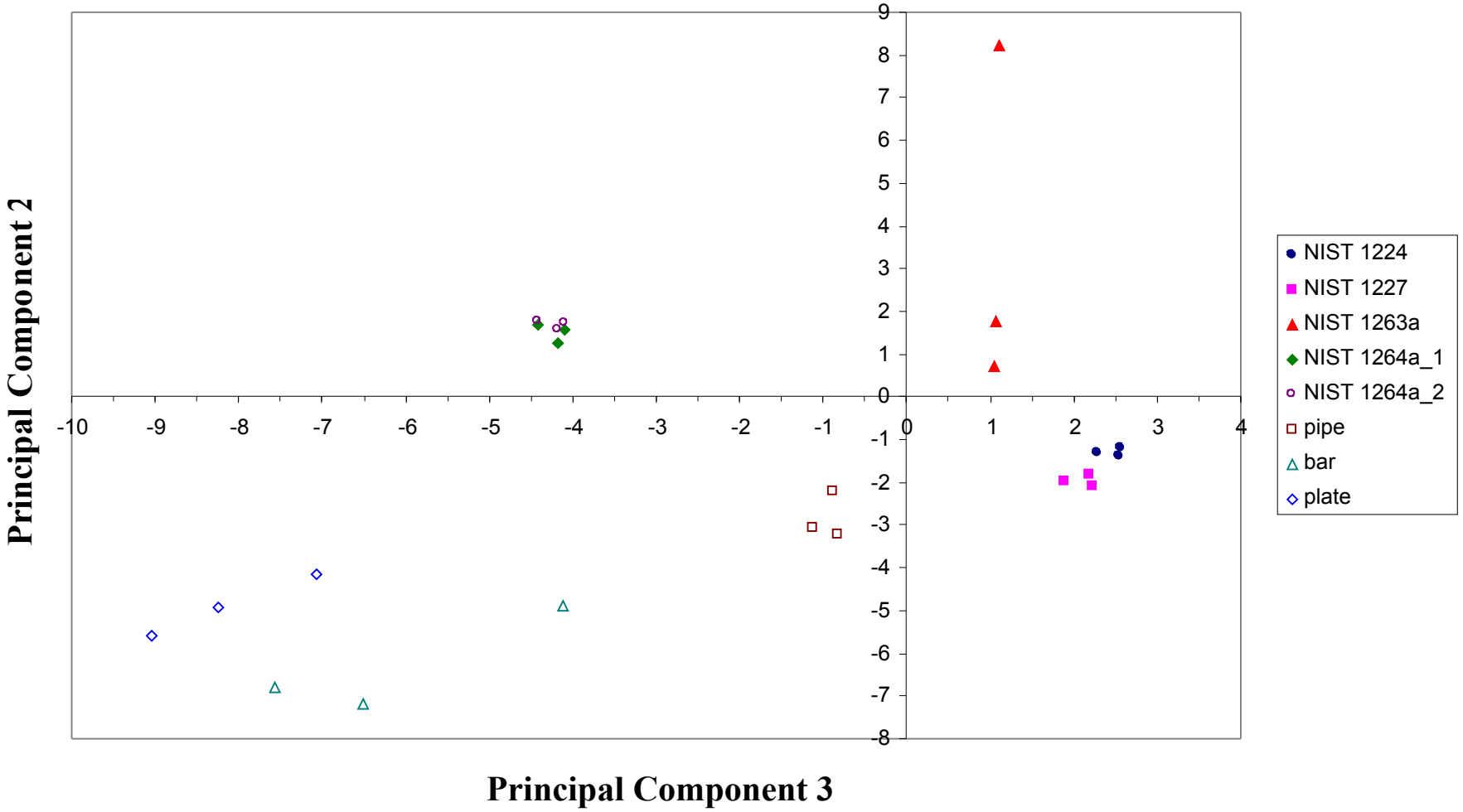

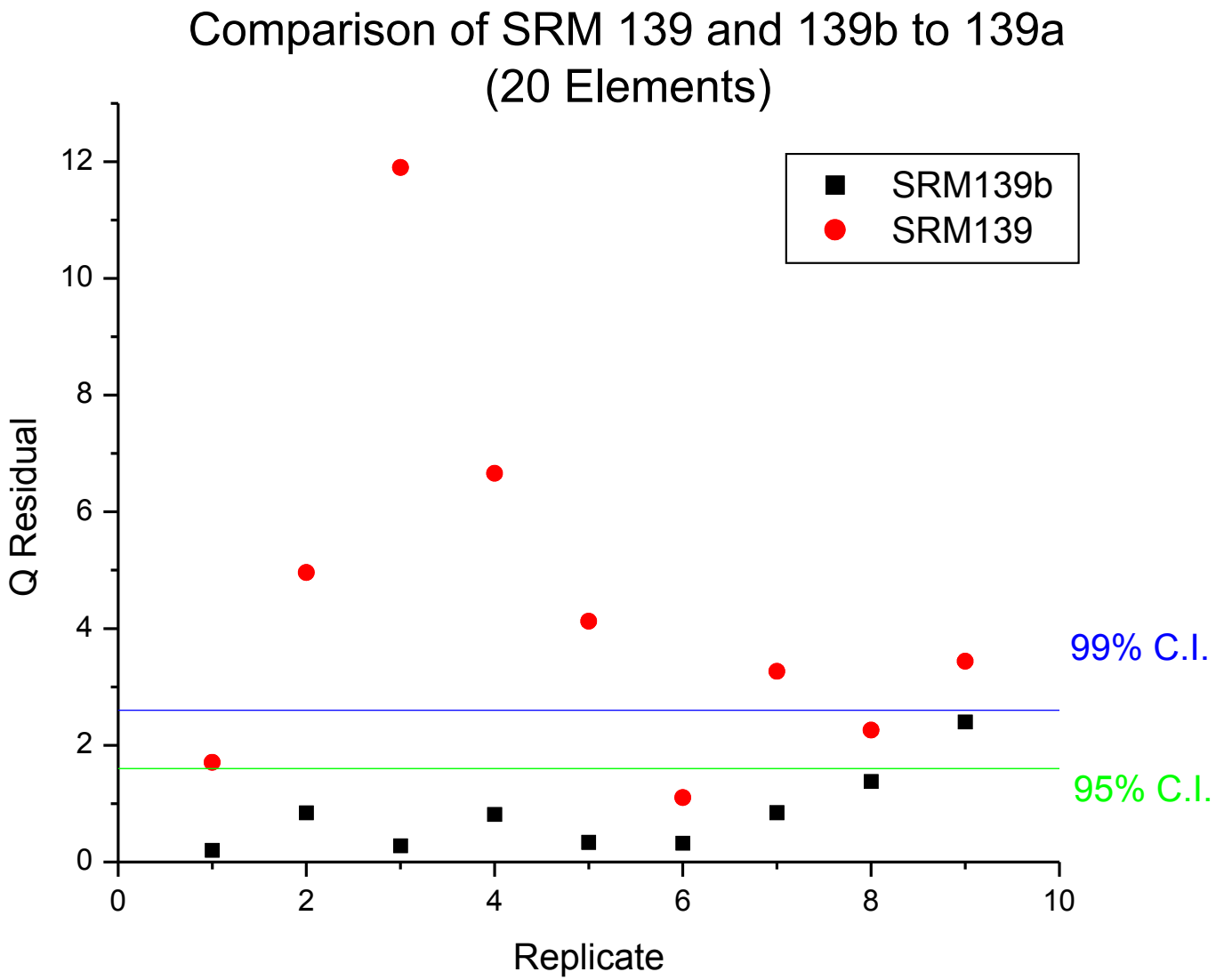
Comparison of SRM 139 and 139b to 139a
(20 Elements)
SRM139b
SRM139
99% C.I.
95% C.I.
Q Residual
Replicate
0
2
4
6
8
10
12

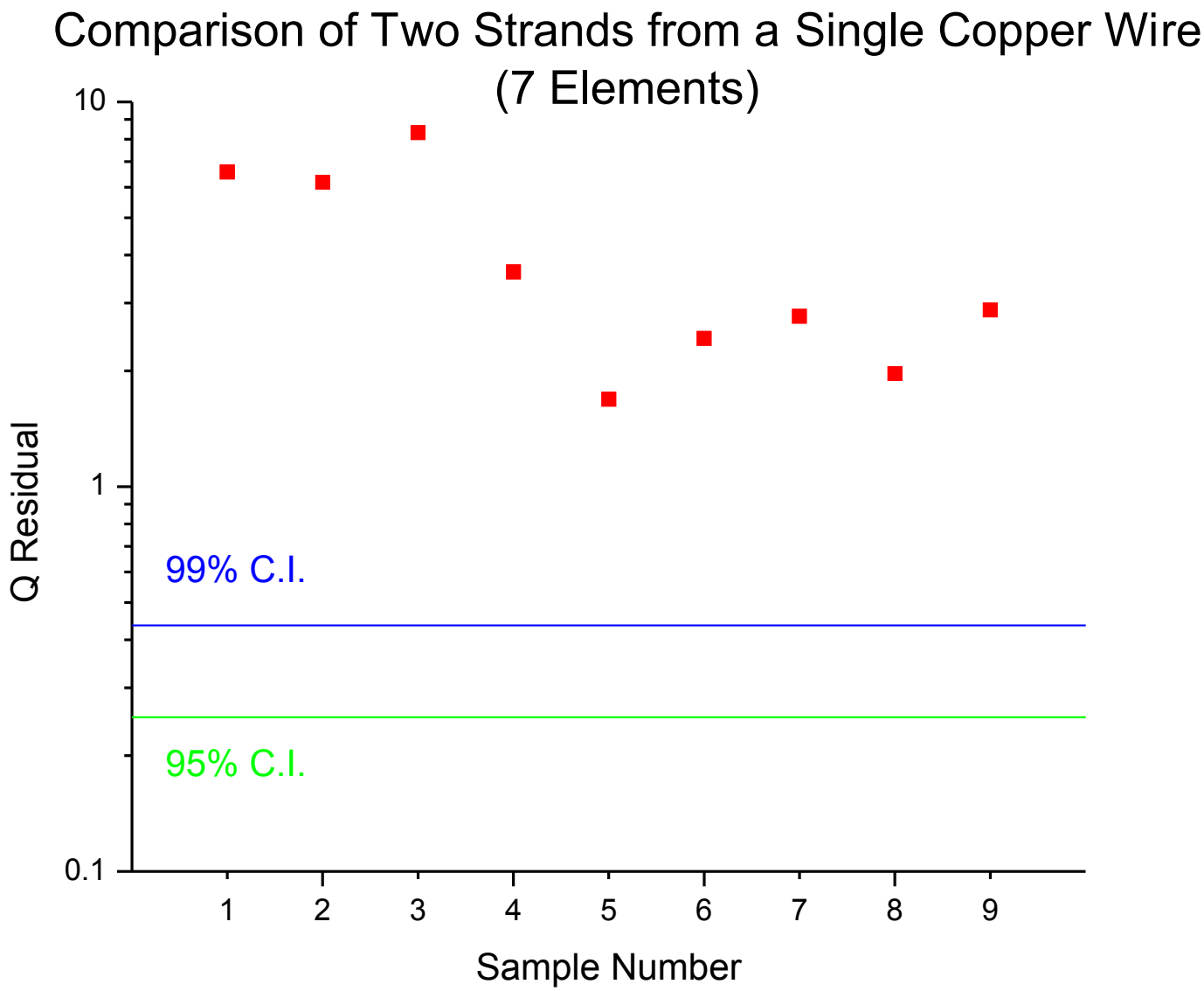
Comparison of Two Strands from a Single Copper Wire
(7 Elements)
10
1
0.1
Q Residual
99% C.I.
95% C.I.
1
2
3
4
5
6
7
8
9
Sample Number

Copper Wire Comparison